

Gamma-ray emission from the Seyfert galaxy NGC 4151 and multi-messenger implications for ultra-fast outflows

E. Peretti^{1,2*}, G. Peron^{2,3†}, F. Tombesi^{4,5,6,7,8}, A. Lamastra⁵, F. G. Saturni^{5,9}, M. Cerruti² and M. Ahlers¹

¹Niels Bohr International Academy, Niels Bohr Institute, University of Copenhagen, Blegdamsvej 17, DK-2100 Copenhagen, Denmark

²Université Paris Cité, CNRS, Astroparticule et Cosmologie, 10 Rue Alice Domon et Léonie Duquet, F-75013 Paris, France

³INAF - Astrophysical Observatory of Arcetri, Largo E. Fermi 5, 50125 Florence, Italy

⁴Physics Department, Tor Vergata University of Rome, Via della Ricerca Scientifica 1, 00133 Rome, Italy

⁵INAF – Astronomical Observatory of Rome, Via Frascati 33, 00078 Monte Porzio Catone (RM), Italy

⁶INFN – Rome Tor Vergata, Via della Ricerca Scientifica 1, 00133 Rome, Italy

⁷Department of Astronomy, University of Maryland, College Park, MD 20742, USA

⁸NASA Goddard Space Flight Center, Code 662, Greenbelt, MD 20771, USA

⁹ASI – Space Science Data Center, Via del Politecnico snc, 00133 Rome, Italy

8 November 2023

ABSTRACT

The enhanced activity typical of the core of Seyfert galaxies can drive powerful winds where high-energy phenomena can occur. In spite of their high power content, the number of such non-jetted active galactic nuclei (AGN) detected in γ rays is very limited. In this Letter, we report the identification and measurement of the γ -ray flux from NGC 4151, a Seyfert galaxy located at about 15.8 Mpc. The source is known for hosting ultra-fast outflows (UFOs) in its innermost core through X-ray spectroscopic observations, thereby becoming the first UFO host ever recognized in γ rays. UFOs are mildly relativistic, wide opening angle winds detected in the innermost parsecs of active galaxies where strong shocks can develop. We interpret the γ -ray flux as a result of diffusive shock acceleration at the wind termination shock of the UFO and inelastic hadronic collisions in its environment. Interestingly, NGC 4151 is also spatially coincident with a weak excess of neutrino events identified by the IceCube neutrino observatory. We compute the contribution of the UFO to such a neutrino excess and we discuss other possible emission regions such as the AGN corona.

Key words: gamma rays – neutrinos – particle acceleration – active galaxies – cosmic rays

1 INTRODUCTION

Ultra-fast outflows (UFOs) have been discovered through observations of highly blue-shifted Fe XXV and Fe XXVI K-shell absorption lines in the X-ray spectra of active galactic nuclei (AGN) and quasars (Chartas et al. 2002, 2003, 2009; Pounds et al. 2003; Dadi et al. 2005; Markowitz et al. 2006; Braito et al. 2007; Cappi et al. 2009; Reeves et al. 2009; Giustini et al. 2011; Gofford et al. 2011; Lobban et al. 2011; Dauser et al. 2012). In particular, the definition of UFOs was first adopted in order to uniquely identify AGN-driven outflows featuring high ionization level and blueshifted lines with associated velocity $\gtrsim 10^4$ km s⁻¹ (Tombesi et al. 2010). A systematic search performed in Tombesi et al. (2010) showed that UFOs are common in nearby ($z \lesssim 0.1$) Seyfert galaxies with a detection fraction $\gtrsim 40\%$. Moreover, a photo-ionization modeling performed in Tombesi et al. (2011) allowed the authors to constrain the typical UFO velocity in the range $u \sim 0.03c - 0.3c$. In addition, Tombesi et al. (2012) estimated that the typical distance of UFOs from the central supermassive black hole (SMBH) is of the order of sub-parsec scales and, in the same work, the typical val-

ues for mass loss rate ($\dot{M} \sim 0.01 - 10 M_{\odot} \text{ yr}^{-1}$) and kinetic power ($\dot{E}_{\text{kin}} = \dot{M} u^2 / 2 \sim 10^{41} - 10^{46}$ erg s⁻¹) were also derived.

UFOs could originate from accretion disc winds launched close to the central SMBH in AGN (Tombesi et al. 2010; Tombesi et al. 2013; Tombesi et al. 2015; Gofford et al. 2013; Laurenti et al. 2021). They are indeed mildly relativistic flows characterized by a wide opening angle (Nardini et al. 2015), typically observed in the nearest parsecs from the SMBH (see also Laha et al. 2021, for a recent review). Similar to other astrophysical diverging flows, UFOs can feature a bubble structure (Faucher-Giguère & Quataert 2012) characterized by an inner wind termination shock and an outer forward shock (Zubovas & King 2012; Costa et al. 2014).

Recently, Peretti et al. (2023) (hereafter referred to as P23) studied the possibility of accelerating particles at the wind termination shock of UFOs. In fact, ideal conditions for diffusive shock acceleration (DSA) of cosmic rays (CRs) can be found at this shock with a maximum proton energy as high as a few EeV. Therefore, UFOs are promising candidate sources of ultra-high-energy CRs. In addition, copious inelastic collisions of CRs with gas (pp) and radiation (p γ) are expected to take place in the UFO due to the extreme radiation field and the high gas density. Therefore, UFOs are expected to be bright high-energy (HE) γ -ray and neutrino sources. The γ -ray flux can escape freely for energies below ~ 100 GeV, while at higher

* E-mail: enrico.peretti.science@gmail.com

† E-mail: giada.peron@inaf.it

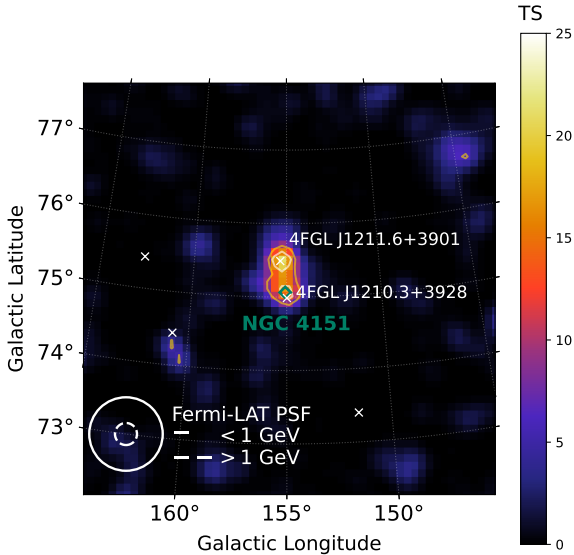


Figure 1. Test statistics (TS) map in the region of NGC 4151 after the subtraction of all background sources except for 4FGL J1211.6+3901 and 4FGL J1210.3+3928. The 4FGL point sources are indicated as white crosses while the position of NGC 4151 as given in SIMBAD is indicated as a green diamond. The yellow and white contours refer to 9 and 20 TS, respectively.

energies the UFO environment can become optically thick due to the strong radiation field associated to the AGN itself. A first tailored study to investigate the γ -ray emission from UFOs was endeavored by the Fermi-LAT Collaboration (Ajello et al. 2021), who carried out a stacking analysis on 11 UFOs. Their result confirmed that UFOs are γ -ray emitters but the employed stacking technique prevents to have clear constraints on the spectrum of these sources. Therefore, UFOs add to the list of potential γ -ray production sites in Seyfert galaxies, where typically star forming regions, weak jets, and galaxy-scale outflows were considered.

In this Letter, we target NGC 4151, a Seyfert 1.5 galaxy (Osterbrock & Koski 1976) located at a distance $D_L \approx 15.8$ Mpc (Yuan et al. 2020) known for hosting an UFO through X-ray observations. We unveil the γ -ray emission from 100 MeV to ~ 100 GeV in the direction of the galaxy and we argue its association with NGC 4151. We interpret the detected γ -ray flux and spectral shape in the context of the theoretical model developed in P23 and we show that the scenario of DSA at the wind termination shock of the UFO is able to explain the observations.

2 FERMI-LAT OBSERVATIONS

We analyzed the data accumulated for more than 14 years by the Fermi-LAT in the energy range 100 MeV–1 TeV. We adopted a standard pipeline using source-type events (evclass=128) with the most stringent cuts on the data quality (DATA_QUAL==1 && LAT_CONFIG==1), reconstructed both in the front and in the back of the detector (evtype=3) and with maximum zenith angle 90° . The null hypothesis of our statistical test has been constructed in the following way: we started from a source model (SM) comprised of all sources from the 4FGL-DR3 source catalog (Abdollahi et al. 2022)¹ within 20° from the center $(l_0, b_0) = (155^\circ, 75^\circ)$ of our

region of interest (see Fig. 1). We combined it with the Galactic (gll_iem_v07) and extra-galactic (iso_P8R3_SOURCE_V3_V1) diffuse γ -ray backgrounds provided by the Fermi-LAT Collaboration². We optimized the 4FGL sources in the SM on the 14-year data, using catalog parameters as initial seed and then we fitted the parameters of the diffuse components. After the optimization of the background sources, we searched for emission in the direction of NGC 4151³. We found two 4FGL sources near the location of NGC 4151⁴ and within the point-spread function (PSF) of the LAT instrument ($\geq 0.5^\circ$): 4FGL J1210.3+3928 (hereafter referred to as SRC-1) and 4FGL J1211.6+3901 (hereafter referred to as SRC-2). Within the Fermi-LAT catalog, both sources were previously associated to blazars, due to their spatial coincidence with 1E 1207.9+3945 and FIRST J121134.2+390053 respectively. However, the former is located within 5 arc-minutes from NGC 4151 making a clear separation of the two sources extremely challenging given the extension of the Fermi-LAT PSF. We investigated the morphology and location of SRC-1 and SRC-2 by removing them from the SM and by fitting their position and extension. We found two point-like sources, with the following best-fit positions: SRC-1 $(l_*, b_*) = (154.91 \pm 0.04, 75.02 \pm 0.03)^\circ$ and SRC-2 $(l_*, b_*) = (155.28 \pm 0.03, 75.49 \pm 0.02)^\circ$. Since the two sources are well separated, in what follows we report only the fit results of SRC-1, while we refer the interested reader to Appendix B for best fit parameters of SRC-2. In addition, we demonstrated, that the nearby source, SRC-2, does not affect the photon flux and the spectral shape of SRC-1 (see Appendix B).

We modeled the emission of SRC-1 with a power-law spectrum $N_0(E/E_0)^{-\alpha}$ normalized at the pivot energy $E_0 = 1$ GeV. The resulting significance is 5.52σ with best-fit normalization $N_0 = (1.3 \pm 0.2) \cdot 10^{-10} \text{ GeV}^{-1} \text{ cm}^{-2} \text{ s}^{-1}$ and spectral index $\alpha = 2.39 \pm 0.18$. The resulting γ -ray luminosity in the energy band 0.1–100 GeV is $L_\gamma \approx 3.7 \cdot 10^{40} \text{ erg s}^{-1}$, which is a fraction $\sim 0.04\%$ of the bolometric luminosity, $L_{\text{bol}} \approx 10^{44} \text{ erg s}^{-1}$ (Crenshaw & Kraemer 2007).

We critically assessed the emission of SRC-1 by testing the hypothesis of blazar-dominated flux with an accurate multi-wavelength spectral modeling and we refer the interested reader to Appendix A for additional details. From our analyses we concluded that the spectrum of SRC-1 is more likely associated to the UFO in NGC 4151 than the blazar. Our results are supported by general observations of extremely-high synchrotron peak (EHSP) blazars, namely those blazars characterised by a synchrotron emission peaked at frequencies larger than 10^{17} Hz and average spectral index of 1.90 ± 0.17 in the MeV-GeV energy band (Foffano et al. 2019; Arsioli et al. 2020) (see Fig. A1). In particular, the soft spectral slope α can hardly represent the emission of an EHSP such as 1E 1207.9+3945, which features the synchrotron peak around 15 keV ($\sim 10^{18}$ Hz) (Maselli et al. 2008).

3 MODELING THE UFO IN NGC 4151

Seyfert 1 galaxies host an active core where the absorption column and/or the dusty torus alignment with the line of sight allows for the optical broad-emission lines to be directly observed and for the X-rays to be also directly observable from the corona surrounding

¹ While writing this manuscript, a new version of the Fermi-LAT catalog (DR4, Ballet et al. 2023, based on 14 years of observations) was announced. We verified that none of the newly identified sources are localized within 5 degrees from NGC 4151, thus they do not influence our analysis.

² <https://fermi.gsfc.nasa.gov/ssc/data/access/lat/BackgroundModels.html>

³ An indication for γ -ray emission (4.2σ) coincident with the position of NGC 4151 was already reported in the previous analysis of Ajello et al. (2021), based on data with a 11-year-long exposure.

⁴ Simbad catalog coordinates of NGC 4151: $(l, b) = (155.08, 75.06)^\circ$

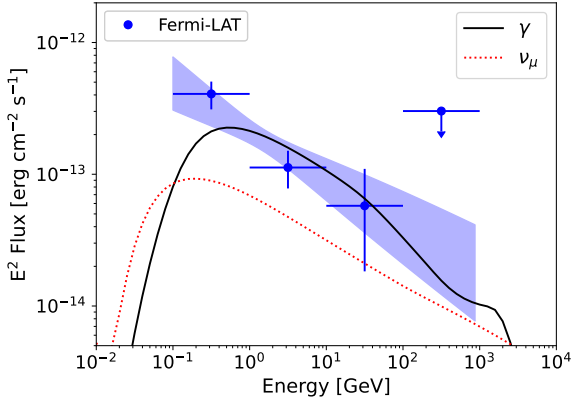


Figure 2. Observed γ -ray flux compared with the multimessenger model prediction. Data points (cyan) are shown along with the 1σ uncertainty band. The thick black line represents the predicted γ -ray flux while the dotted red curve is the associated per-flavor neutrino flux.

the SMBH. NGC 4151 is one of the first Seyfert galaxies ever discovered (Seyfert 1943) and it features intermediate spectral properties between a Seyfert 1 and Seyfert 2 (Osterbrock & Koski 1976). In addition, NGC 4151 hosts an X-ray UFO which has been previously detected and investigated in detail.

In order to constrain the observable properties of the UFO hosted in NGC 4151 we considered two sets of observations performed respectively by *XMM-Newton* (Tombesi et al. 2010, 2011, 2012) and *Suzaku* X-ray satellites (Gofford et al. 2013, 2015), summarized in Table 1. The X-ray luminosity in the 2-10 keV band, L_X , and the wind speed, u , show good agreement among the two measurements. X-ray observations allow upper/lower limits to be placed on the UFO fast wind location given the measured parameters of the absorbing gas, albeit with large uncertainties. The maximum radius, $R_{\text{obs}}^{\text{max}}$, up to which high velocity gas is detected shows a wide range of values from a hundred gravitational radii up to parsec scale, while for the minimum radius, $R_{\text{obs}}^{\text{min}}$, consistent measurements are obtained at around a few tens of gravitational radii. Similarly, the measured min (max) values for the mass loss rate, \dot{M}_{min} (\dot{M}_{max}), and kinetic power, $\dot{E}_{\text{kin}}^{\text{min}}$ ($\dot{E}_{\text{kin}}^{\text{max}}$), show large uncertainties.

Even if affected by relatively large uncertainties in its location, mass-loss rate and power, the UFO physical parameters are extremely useful to identify the range of allowed values to be considered for the following model.

3.1 Cosmic ray acceleration and transport model

The UFO is considered as a spherically symmetric and energy-conserving outflow featuring a bubble structure. The system is characterized as follows: 1) a wind shock (located at R_{sh}) separates the innermost fast cool wind of constant velocity from the hot shocked wind, where the wind speed decreases as $\sim r^{-2}$; 2) a contact discontinuity (located at R_{cd}) separates the hot shocked wind from the shocked ambient medium; 3) an outer forward shock (located at R_{fs}) bounds the system.

The main macroscopic parameters of an UFO are the mass loss rate, \dot{M} , and the terminal wind speed u . The evolution, size and density profile of a system with given \dot{M} and u are set once one fixes the age t_{age} and the external medium density n_0 (Weaver et al. 1977; Koo & McKee 1992a,b; Faucher-Giguère & Quataert 2012). Following P23, the upstream magnetic field pressure is inferred as a small fraction $\epsilon_B = 0.1$ of the ram pressure, while the downstream one is the result of compression of the perpendicular components

Table 1. Parameters of the UFO in NGC 4151 as inferred from X-ray observations with *XMM-Newton* or *Suzaku*.

Parameter	<i>XMM-Newton</i> [†]	<i>Suzaku</i> [*]	Unit
L_X	3.0	2.0	$10^{42} \text{erg s}^{-1}$
u	0.106	0.055	c
$R_{\text{obs}}^{\text{min}} / R_{\text{obs}}^{\text{max}}$	$10^{-4} / 4 \cdot 10^{-4}$	$2 \cdot 10^{-4} / 0.4$	pc
$\dot{M}_{\text{min}} / \dot{M}_{\text{max}}$	0.0025 / 0.04	0.0006 / 0.25	$M_{\odot} \text{yr}^{-1}$
$\dot{E}_{\text{kin}}^{\text{min}} / \dot{E}_{\text{kin}}^{\text{max}}$	0.8 / 12.6	0.05 / 25.1	$10^{42} \text{erg s}^{-1}$

[†] Tombesi et al. (2010, 2011, 2012); ^{*} Gofford et al. (2013, 2015)

of the upstream field at the wind termination shock. The magnetic field is also assumed to be characterized by a coherence length, $l_c = 0.01$ pc. The AGN photon field is computed following Marconi et al. (2004) with an X-ray luminosity within the range inferred from observations. The photon number density is assumed to decay as the square of the distance from the SMBH. We also consistently account for the infrared thermal component produced by a dusty torus (Mullaney et al. 2011).

DSA takes place at the wind termination shock, R_{sh} , where a high Mach number can be found, while particles freely escape once they reach the forward shock. As in P23 we solve the stationary space-dependent transport equation in the whole system. The solution at R_{sh} can be expressed in the following compact form:

$$f_{\text{sh}}(p) = C \left(\frac{p}{p_{\text{inj}}} \right)^{-s} \exp[-\Gamma_{\text{cut}}(p)], \quad (1)$$

where s is the slope of the injected particles – assumed here as a free parameter – C is a normalization constant set by $\xi_{\text{CR}} \approx 0.1$ (ratio between the CR pressure and the ram pressure at the wind shock) and Γ_{cut} is the cut-off function depending on the size of the system and the transport properties therein. CR interactions with gas (pp) and radiation (p γ) produce hadronic emission of γ -rays and neutrinos (our computational method is based on Kelner et al. 2006; Kelner & Aharonian 2008). We refer the interested reader to P23 for additional details on the acceleration and transport model.

3.2 Application to NGC 4151

In what follows we specialize our calculations to the case of NGC 4151. In agreement with the observations, we consider an UFO of velocity $u \approx 0.1c$ with a mass loss rate $\dot{M} \approx 2 \cdot 10^{-2} M_{\odot} \text{yr}^{-1}$. We explore a typical range of external density, $10^3 \lesssim n_0 / \text{cm}^{-3} \lesssim 10^6$ (see P23), and we derive the associated t_{age} and slope of the accelerated particles (s) requiring the predicted γ rays to match the observations. Interestingly, the estimates of the emission size inferred from the X-rays provide a constraint on the available parameter space. We find that a spectral index $s = 4.4$ is favoured in order to properly fit the γ -ray flux. We notice that, different from P23 and Ajello et al. (2021), the soft γ -ray spectrum observed requires an injection slope softer than the standard prediction of DSA. This can be possibly motivated by a drift of the scattering centers in the downstream region of the shock (Caprioli et al. 2020). Alternative scenarios where the proton injection slope is harder, say $s = 4$, could be a possible alternative if a leptonic cascade were contaminating the GeV range resulting in a softening of the observed spectrum. We leave a detailed leptonic modeling to future investigations.

In general, we obtained that different combinations of n_0 and t_{age} can well explain the γ -ray flux. Despite the parameter degeneracy, we identify three main configurations of the UFO that are compatible with the observations: A) sub-parsec-sized; B) parsec-sized; C)

Table 2. Best fit parameters for the possible realizations of the UFO in NGC 4151.

Model	n_0 [cm ⁻³]	t_{age} [yr]	$R_{\text{sh}} - R_{\text{fs}}$ [pc]	E_{max} [10 ² PeV]
A	10 ⁵	3.0 · 10 ²	0.1 – 0.5	1.63
B	10 ⁴	2.5 · 10 ³	0.6 – 3.0	3.68
C	10 ³	1.4 · 10 ⁴	2.5 – 13	2.75

multi-parsec-sized. Table 2 reports the specific values of the parameters relative to each configuration with the associated maximum energy that in all cases is $\gtrsim 10^2$ PeV. We observe that scenarios with $n_0 \gg 10^5 \text{ cm}^{-3}$ are disfavoured since they would result in a time variability of the UFO shorter than the Fermi-LAT observational time (see also figure A3 in Appendix A) and in a size of the order of 10^{-2} pc. Such a size is in tension with the $R_{\text{obs}}^{\text{max}}$ inferred from observations with Suzaku.

Figure 2 shows the γ -ray and per-flavour neutrino spectra of our UFO model A as solid blue and dotted red lines, respectively. Model B and C do not differ from model A in the energy range where data are present. The emission is dominated by pp interactions in the shocked ambient medium layer (see also Mou et al. 2015, for similar results) and follows the injection spectrum of the CR population. The γ -ray spectrum is attenuated by $\gamma\gamma$ interactions (Aharonian 2004) in the AGN photon field. As can be seen in the figure, our UFO model reproduces the inferred γ -ray SED well within the 1σ uncertainty band. The predicted neutrino emission of the UFO can be tested by neutrino observatories, such as IceCube (Abbasi et al. 2022). IceCube’s sensitivity for time-integrated muon-neutrino emission from a source located at declination $\delta \simeq 39^\circ$ is $E^2 F_{\nu_\mu + \bar{\nu}_\mu}(E) \simeq (4 - 8) \cdot 10^{-13} \text{ TeV cm}^{-2} \text{ s}^{-1}$ at a reference energy of 1 TeV for spectral indices $\gamma = 2.0 - 3.2$. As shown in Fig. 2, at around 1 TeV the predicted per-flavor neutrino flux from the UFO is at the level of $E^2 F_{\nu_\mu + \bar{\nu}_\mu} \simeq 5 \cdot 10^{-15} \text{ TeV cm}^{-2} \text{ s}^{-1}$, *i.e.* two orders of magnitude below IceCube’s sensitivity.

4 DISCUSSION

NGC 4151 is a unique laboratory to probe wind launching and acceleration processes at different energy regimes. In fact, its central engine is known to host a potential multi-phase outflow that produces a series of variable absorption features from the X-rays (2 – 10 keV; Schurch & Warwick 2002; Tombesi et al. 2010; Gofford et al. 2013) to the near infrared (He I; Wildy et al. 2016). The investigation of such processes in this source – as already done in other nearby AGN, such as Mrk 231 (Feruglio et al. 2015) – may thus contribute to shed additional light on the nature of multi-phase AGN outflows, that is still largely unconstrained so far (Cicone et al. 2018). In conjunction with the analysis of shock-induced γ -rays, the search for neutrino emission from this NGC 4151 constitutes a new powerful tool for a complementary investigation.

While the UFO model of NGC 4151 can successfully account for the observed γ -ray spectrum, it predicts neutrino emission that falls far below the sensitivity of current neutrino observatories. However, there exist alternative hadronic models of AGN that would allow to boost the neutrino emission compared to the relatively low γ -ray flux. These models feature CR interactions in a region that is highly opaque to GeV γ -rays, such as the AGN corona (see e.g. Inoue et al. 2019, 2020; Murase et al. 2020; Eichmann et al. 2022; Murase 2022) or a shocked environment by a combination of a successful and failed line driven winds close to the accretion disk (Inoue et al. 2022). In particular, these models have been invoked to explain the

multimessenger spectra of the Seyfert 2 galaxy NGC 1068 where IceCube finds compelling evidence for neutrino emission (Abbasi et al. 2022). Interestingly, NGC 4151 is located at a distance of only 0.18° from the fourth most significant hot spot in the search for northern neutrino point sources with spectral index $\alpha_\nu = 2.5$ in the same IceCube analysis (see supplement of Abbasi et al. 2022). In what follows, we estimate possible upper limits for the neutrino emission in the AGN corona of NGC 4151 considering the most optimistic scenario provided by calorimetric conditions.

We assume that a non-thermal population of protons – in approximate equipartition with the X-rays – is injected in the corona environment with a total luminosity L_{CR} as large as a fraction $\eta_{\text{CR}} \lesssim 3\%$ of the AGN bolometric luminosity L_{bol} . Following Inoue et al. (2019) we assume that protons are injected with a spectral slope as hard as $\sim E^{-2}$ and a maximum energy $E'_{\text{max}} \approx 1$ PeV, where the maximum energy is in agreement with the assumed X-ray luminosity. Adopting the notation of Murase et al. (2016), we can estimate an upper limit on the per-flavor neutrino flux in the calorimetric limit as:

$$E^2 F_{\nu_\alpha} \lesssim \frac{K}{4(1+K)} \frac{\chi \eta_{\text{CR}} L_{\text{bol}}}{4\pi D_L^2}, \quad (2)$$

where $\chi \equiv 1/\ln(E'_{\text{max}}/\text{GeV})$ is a normalization factor assuming E^{-2} CR spectra between 1 GeV and E'_{max} and $K \approx 2(1)$ for pp ($p\gamma$) interactions. Assuming pp interactions, this gives an upper limit for NGC 4151 of:

$$E^2 F_{\nu_\alpha} \lesssim 5 \cdot 10^{-13} \left(\frac{\eta_{\text{CR}}}{0.03} \right) \left(\frac{\chi}{0.05} \right) \left(\frac{L_{\text{bol}}}{10^{44} \text{ erg s}^{-1}} \right) \frac{\text{TeV}}{\text{cm}^2 \text{ s}}. \quad (3)$$

This order of magnitude estimate illustrates that, if a neutrino flux was confirmed from NGC 4151 at a level of IceCube’s present sensitivity level (Abbasi et al. 2022), efficient CR acceleration and interactions in the corona could be a plausible scenario. Finally, we notice that stochastic acceleration (Murase et al. 2020) and magnetic reconnection (Drury 2012; Kheirandish et al. 2021) could be alternative acceleration mechanisms in AGN coronae. However, different from DSA, they could allow for injection spectra as hard as $\sim E^{-1}$. In such a scenario, the upper limit set in Equation (3) could be partially relaxed and, in the same parametric configuration, the neutrino flux could be peaking at TeV while being up to one order of magnitude larger in normalization at the peak, thereby in agreement with what has been inferred in Neronov et al. (2023).

5 CONCLUSIONS

In this Letter we report – for the first time – the identification of γ -ray emission from NGC 4151, a nearby (15.8 Mpc) Seyfert 1.5 galaxy. The significance of the detection is 5.5σ and it is supported by the spatial coincidence of the γ -ray excess with the position of NGC 4151 and the associated spectral energy distribution.

This source hosts a mildly-relativistic UFO in its core region detected by Suzaku and XMM-Newton. Thus, we interpret the γ -ray emission in the context of particle acceleration at the wind termination shock of the UFO where γ -rays as well as HE neutrinos are produced via inelastic pp interactions in the shocked ambient medium. We notice, in particular, that the particle acceleration model is well constrained by the parameters obtained from X-ray observations and it is energetically motivated by standard parametric assumptions typical for the test-particle regime, namely the pressure of accelerated particles is $\lesssim 10\%$ of the ram pressure at the shock. We find that particles could reach energies as high as 10^2 PeV in this UFO. We additionally highlight that from the star-formation rate (SFR) inferred for NGC 4151 ($0.25 M_\odot \text{ yr}^{-1}$ Erroz-Ferrer et al. 2015) one can predict

the following γ -ray luminosity $L_{\gamma}^{(\text{SFR})} \approx 2.9 \cdot 10^{38} \text{ erg s}^{-1}$ adopting the SFR-to-gamma correlation typical of star forming galaxies (Kornecki et al. 2020, 2022). Interestingly, such luminosity is more than two orders of magnitude smaller than what we obtain with our measurement: $L_{\gamma} \approx 3.65 \cdot 10^{40} \text{ erg s}^{-1}$. This is a strong and clean indication that the γ -ray emission is related to the AGN activity taking place in NGC 4151. The HE neutrino flux associated to the γ -ray observation is self-consistently computed in the context of the UFO model and we observe that it is about two orders of magnitude below the sensitivity of the IceCube observatory. We note, however, that a recent IceCube analysis found compelling evidence for neutrino emission of the Seyfert 2 galaxy NGC 1068. The same analysis also found indications for neutrino emission in the vicinity of NGC 4151, although with much lower significance. If NGC 4151 was confirmed as a neutrino source at the level of IceCube's present sensitivity, it would imply that NGC 4151 hosts a partially hidden accelerator with relatively low GeV counterpart, *e.g.* close to the accretion disk with γ -ray absorption in the AGN corona. We provide an estimate of the maximum neutrino emission achievable under calorimetric conditions and show that it is consistent with a flux as high as the present IceCube sensitivity level.

While improving our analysis Inoue & Khangulyan (2023) adopted our public preliminary results to propose the jet and the AGN corona as alternative γ -ray emission sites. Interestingly, they also computed a neutrino flux produced in the corona of NGC 4151 and their result is consistent and very close with our upper limits possibly suggesting a calorimetric environment. In this context, there could be also another possible contamination to the γ ray flux coming from a larger scale molecular outflow (see *e.g.* Lamastra et al. 2016; Kraemer et al. 2020), while the star formation, as discussed, is unlikely to contribute.

NGC 4151 is an extremely interesting multi-messenger source and further observational campaigns are of crucial relevance in order to decipher its complex nature. Multi-wavelength observations, could help understanding its constituents and characterize the non-thermal emission regions. In particular, the TeV domain can provide timely and insightful information on the nature of the multi-messenger cosmic accelerator caught on act.

ACKNOWLEDGEMENTS

EP and MA acknowledge support by Villum Fonden (No. 18994). EP was also supported by the European Union's Horizon 2020 research and innovation program under the Marie Skłodowska-Curie grant agreement No. 847523 'INTERACTIONS'. GP was supported by Agence Nationale de la Recherche (grant ANR-21-CE31-0028). FGS was supported by the PRIN MIUR project "ASTRI/CTA Data Challenge" (PI: P. Caraveo), contract 298/2017. EP is grateful to S. Bianchi, P. Padovani, K. Murase, C. Karwin and M. Ajello for insightful discussions.

DATA AVAILABILITY

Fermi-LAT data are publicly available at: <https://fermi.gsfc.nasa.gov/ssc/data/access/>. Our analysis made use of the Fermipy (v.0.17.4) software package (Wood et al. 2018).

REFERENCES

- Abbasi R., et al., 2022, *Science*, 378, 538
 Abdollahi S., et al., 2022, *ApJS*, 260, 53
 Aharonian F. A., 2004. World Scientific Publishing, doi:10.1142/4657
 Ajello M., et al., 2021, *ApJ*, 921, 144
 Arsioli B., Chang Y. L., Musiimenta B., 2020, *MNRAS*, 493, 2438
 Ballet J., et al., 2023, *arXiv e-prints*, p. arXiv:2307.12546
 Braito V., et al., 2007, *ApJ*, 670, 978
 Cappi M., et al., 2009, *A&A*, 504, 401
 Caprioli D., Haggerty C. C., Blasi P., 2020, *ApJ*, 905, 2
 Cerruti M., Zech A., Boisson C., Inoue S., 2015, *MNRAS*, 448, 910
 Chartas G., et al., 2002, *ApJ*, 579, 169
 Chartas G., Brandt W. N., Gallagher S. C., 2003, *ApJ*, 595, 85
 Chartas G., et al., 2009, *ApJ*, 706, 644
 Cicone C., et al., 2018, *Nature Astronomy*, 2, 176
 Costa T., Sijacki D., Haehnelt M. G., 2014, *MNRAS*, 444, 2355
 Crenshaw D. M., Kraemer S. B., 2007, *Astrophys. J.*, 659, 250
 Dadina M., et al., 2005, *A&A*, 442, 461
 Dauser T., et al., 2012, *MNRAS*, 422, 1914
 Drury L. O., 2012, *MNRAS*, 422, 2474
 Eichmann B., et al., 2022, *ApJ*, 939, 43
 Erroz-Ferrer S., et al., 2015, *MNRAS*, 451, 1004
 Faucher-Giguère C.-A., Quataert E., 2012, *MNRAS*, 425, 605
 Feruglio C., et al., 2015, *A&A*, 583, A99
 Foffano L., et al., 2019, *MNRAS*, 486, 1741
 Giustini M., et al., 2011, *A&A*, 536, A49
 Gofford J., et al., 2011, *MNRAS*, 414, 3307
 Gofford J., et al., 2013, *MNRAS*, 430, 60
 Gofford J., et al., 2015, *MNRAS*, 451, 4169
 Inoue Y., Khangulyan D., 2023, *arXiv e-prints*, p. arXiv:2304.04138
 Inoue Y., Khangulyan D., Inoue S., Doi A., 2019, *ApJ*, 880, 40
 Inoue Y., Khangulyan D., Doi A., 2020, *ApJ*, 891, L33
 Inoue S., Cerruti M., Murase K., Liu R.-Y., 2022, *arXiv:2207.02097*,
 Kelner S. R., Aharonian F. A., 2008, *Phys. Rev. D*, 78
 Kelner S. R., Aharonian F. A., Bugayov V. V., 2006, *Phys. Rev. D*, 74, 034018
 Kheirandish A., Murase K., Kimura S. S., 2021, *ApJ*, 922, 45
 Koo B.-C., McKee C. F., 1992a, *ApJ*, 388, 93
 Koo B.-C., McKee C. F., 1992b, *ApJ*, 388, 103
 Kornecki P., et al., 2020, *A&A*, 641, A147
 Kornecki P., et al., 2022, *A&A*, 657, A49
 Kraemer S. B., et al., 2020, *MNRAS*, 493, 3893
 Laha S., et al., 2021, *Nature Astronomy*, 5, 13
 Lamastra A., et al., 2016, *A&A*, 596, A68
 Laurenti M., et al., 2021, *A&A*, 645, A118
 Lobban A. P., et al., 2011, *MNRAS*, 414, 1965
 Marconi A., et al., 2004, *MNRAS*, 351, 169
 Markowitz A., Reeves J. N., Braito V., 2006, *ApJ*, 646, 783
 Maselli A., et al., 2008, *A&A*, 479, 35
 Morris S. L., et al., 1991, *ApJ*, 380, 49
 Mou G., Yuan F., Gan Z., Sun M., 2015, *ApJ*, 811, 37
 Mullaney J. R., et al., 2011, *MNRAS*, 414, 1082
 Murase K., 2022, *arXiv:2211.04460*,
 Murase K., Guetta D., Ahlers M., 2016, *Phys. Rev. Lett.*, 116, 071101
 Murase K., Kimura S. S., Mészáros P., 2020, *Phys. Rev. Lett.*, 125, 011101
 Nardini E., et al., 2015, *Science*, 347, 860
 Neronov A., et al., 2023, *arXiv e-prints*, p. arXiv:2306.09018
 Osterbrock D. E., Koski A. T., 1976, *MNRAS*, 176, 61P
 Peretti E., et al., 2023, *MNRAS*, 526, 181
 Pounds K. A., et al., 2003, *MNRAS*, 342, 1147
 Reeves J. N., et al., 2009, *ApJ*, 701, 493
 Schurch N. J., Warwick R. S., 2002, *MNRAS*, 334, 811
 Seyfert C. K., 1943, *ApJ*, 97, 28
 Stocke J. T., et al., 1985, *ApJ*, 298, 619
 Tavecchio F., Maraschi L., Ghisellini G., 1998, *ApJ*, 509, 608
 Tombesi F., et al., 2010, *A&A*, 521, A57
 Tombesi F., et al., 2011, *ApJ*, 742, 44
 Tombesi F., Cappi M., Reeves J. N., Braito V., 2012, *MNRAS*, 422, L1
 Tombesi F., et al., 2013, *MNRAS*, 430, 1102
 Tombesi F., et al., 2015, *Nature*, 519, 436
 Weaver R., McCray R., Castor J., Shapiro P., Moore R., 1977, *ApJ*, 218, 377
 Wildy C., et al., 2016, *MNRAS*, 461, 2085
 Wood M., et al., 2018, *PoS, ICRC2017*, 594
 Yuan W., et al., 2020, *ApJ*, 902, 26
 Zubovas K., King A., 2012, *ApJ*, 745, L34

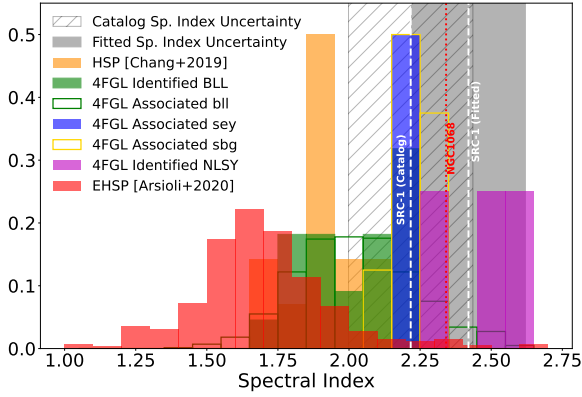


Figure A1. Distribution of spectral indexes of different source populations as reported in the 4FGL source catalog (Abdollahi et al. 2022). The fitted spectral index of SRC-1 is also plotted as reported by the catalog and by our analysis (dashed white lines) along with its associated uncertainty (grey areas). The spectral index of NGC 1068 is also indicated in red.

APPENDIX A: SRC-1 IDENTIFICATION

The blazar 1E 1207.9+3945 (a BL Lacertae object at $z=0.62$, Morris et al. 1991) is a background source for NGC 4151, and it is important to quantify its possible contribution in the LAT spectrum. We investigate in this section what would be the consequences of attributing the LAT signal from SRC-1 to this blazar. We start by comparing in Figure A1 the spectral index of SRC-1 with the spectral indexes of the identified BL Lacertae objects in the 4FGL catalog. As one can see from the histogram, the soft LAT spectrum would make this source an outlier among the blazar population. The association of the LAT SRC-1 with 1E 1207.9+3945 is even more problematic if we look at its multi-wavelength emission. Its spectral energy distribution (SED) shows a synchrotron (SYN) peak at around 10^{18} Hz, classifying the source as extremely-high-frequency-peaked-BL Lac object (EHBL, see e.g. Foffano et al. 2019). An EHBL with a second SED peak below 100 MeV is extremely rare, and this kind of SED can be easily ruled out from a theoretical point of view. Assuming that the emission is primarily leptonic and due to synchrotron-self-Compton (SSC) scattering as typical in HBLs, we can use the analytical formulae derived in Tavecchio et al. (1998) to put constraints on the model parameters. From the equation relating the peaks of the SED component, assuming $\nu_{\text{syn}} = 10^{18}$ Hz, and $\nu_{\text{SSC}} = 10^{22.8}$ Hz, the estimation of the magnetic field in the emitting region is $B = 9.1 \times 10^5 (\delta/10)^{-1}$ G, (with δ the Doppler factor of the emitting region) which is already an unrealistic value, several orders of magnitude larger than what typically constrained in HBLs. The equation relating the peak luminosities gives on the other hand a relatively standard value of $B = 0.04 (\delta/10)^{-3} (\tau/1 \text{ month})^{-1}$ G, (with τ the observed variability time-scale) but it is then clear that it is impossible to reconcile the two values. This simple analytical estimate is thus enough to exclude 1E 1207.9+3945 as the only counterpart of SRC-1. It is then legitimate to ask what can be the maximum contribution of the source to the γ -ray signal. With this goal we model the SED of the source in a leptonic framework (using the code described in Cerruti et al. 2015), assuming model parameters typical for extreme-HBLs ($\delta = 50$, $B = 1$ mG, $R = 3.2 \times 10^{17}$ cm, electrons parametrized as power-law function with index $\alpha = 2$ between $\gamma_{\text{min}} = 300$ and $\gamma_{\text{max}} = 3 \times 10^6$), to evaluate where its γ -ray peak could occur. The SSC model is shown in Figure A2 compared with multiwavelength data collected by several instruments. The modeling is performed on data collected simultaneously by Swift UVOT and XRT (green

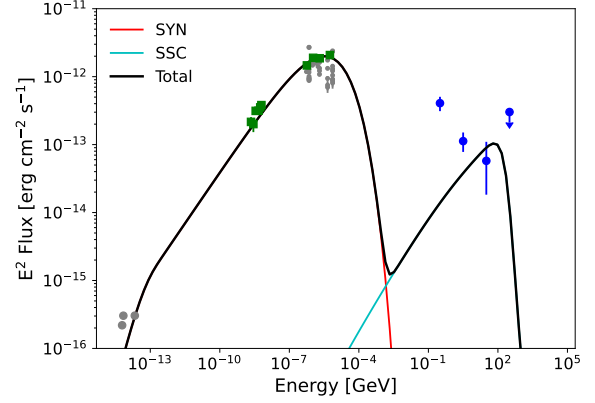


Figure A2. Multiwavelength SSC modeling of the blazar 1E 1207.9+3945. The green data points are from the analysis of Maselli et al. (2008) of Swift UVOT and XRT data. The radio data (grey circles) come from VLA observations (Stoake et al. 1985), while grey points are other asynchronous X-ray observations from Swift and XMM-Newton. The blue points are the Fermi-LAT data points collected in this work.

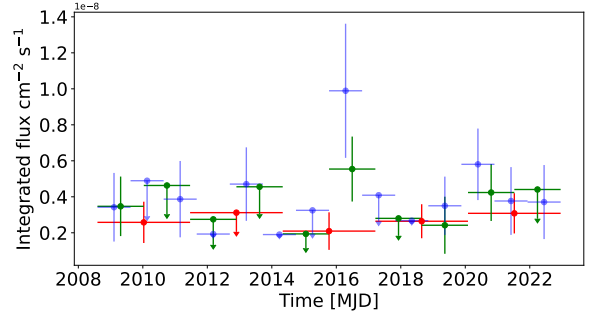


Figure A3. Gamma-ray lightcurve derived by Fermi-LAT for the source SRC-1 in different temporal bins of 1 year (blue), 1.4 years (green) and 2.9 years (red).

square), as reported in (Maselli et al. 2008). Additional flux points (grey dots) collected respectively by VLA, Swift and XMM-Newton and retrieved from the SED builder platform are included for comparison. To avoid source confusion, we excluded data from other X-ray observatories that had an angular resolution bigger than the separation (~ 5 arcmin) between the blazar and NGC 4151. Given that there is no firm γ -ray detection from the source, the model is degenerate, and we present here a solution that maximizes the emission in the LAT band without violating it. As can be seen, 1E 1207.9+3945 could contribute to SRC-1 but only above 10 GeV, while the bulk of the LAT signal with its soft spectral index, can be confidently attributed to NGC 4151.

For interested readers we report in figure A3 the γ -ray lightcurve of SRC-1 obtained with different temporal binning. As one can see, there are no strong indications of time variability in the source.

APPENDIX B: INFLUENCE OF 4FGL J1211.6+3901 (SRC-2)

We run different tests to assess the quality of our detection of SRC-1 (associated with NGC 4151), due to the possible influence of the nearby catalogued source 4FGL J1211.6+3901 (SRC-2). We construct four SMs all including the optimized background sources, as described in the main text, but with different assumption for the con-

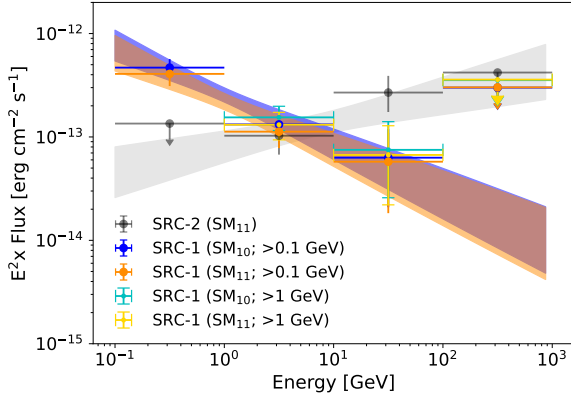


Figure B1. The spectral energy distribution of the blazar 4FGL J1211.6+3901 (SRC-2) and of NGC 4151 (SRC-1) in the different configurations.

Table B1. Significance and spectral parameters of SRC-1 from different source models (SMs) as explained in the main text. The flux normalization N_0 at the pivot energy $E_0 = 1$ GeV is in unit of $10^{-10} \text{ GeV}^{-1} \text{ cm}^{-2} \text{ s}^{-1}$.

energy range	SM	AIC	$\sigma_{\text{SRC-1}}$	N_0	α
> 100 MeV	SM ₁₁	47120.57	5.46	1.3 ± 0.3	2.42 ± 0.2
	SM ₁₀	47153.50	6.57	1.6 ± 0.3	2.48 ± 0.18
	SM ₀₁	47146.45	–	–	–
	SM ₀₀	47192.69	–	–	–
> 1 GeV	SM ₁₁	55732.33	4.53	0.9 ± 0.4	2.18 ± 0.23
	SM ₁₀	55760.94	5.20	1.1 ± 0.4	2.20 ± 0.22
	SM ₀₁	55744.32	–	–	–
	SM ₀₀	55783.43	–	–	–

figuration of the central excess, as follows: SM₀₀ excludes both SRC-1 and SRC-2, SM₁₀ includes only SRC-1, SM₀₁ includes only SRC-2 and SM₁₁ includes both sources. We compute the likelihood of each SM, and compute the significance and spectral shape of SRC-1 in the different configurations. To evaluate which SM is preferred, we use the Akaike information criterion and compute $\text{AIC} = 2k - 2\mathcal{L}$, where k is the number of parameters of the model and \mathcal{L} is the log-likelihood that results from the fit. The model which is favored by the lower AIC is SM₁₁ (highlighted in Table B1), the SM including both sources. We compute the significance of SRC-1 as $\sigma_{\text{SRC-1}} = \sqrt{2(\mathcal{L}_{1j} - \mathcal{L}_{0j})}$, where \mathcal{L}_{ij} are the log-likelihood of the respective SM_{ij}. In the latter we account for the situation where the blazar is included or not to the SM, and for both cases we extract the spectral energy distribution and compute the spectral parameters. We perform this test, both, with γ -rays of energies > 100 MeV and with only those of energies > 1 GeV. At higher energy, the Fermi-LAT point spread function significantly improves, maximizing the chance for separation of the two sources. The resulting spectral parameters and significance are reported in Table B1 along with the AIC values. The significance in all cases is $\geq 5\sigma$, confirming the detection of SRC-1 despite the vicinity of the blazar. The spectral energy distribution for the different configuration are reported in Fig. B1. The spectrum is stable disregarding of the nearby blazar, which is modelled as a power-law of index $\alpha_{\text{SRC-2}} = 1.99 \pm 0.14$ and normalization at 1 GeV of $N_{0,\text{SRC-2}} = 1.15 \pm 0.03 \times 10^{-10} \text{ GeV}^{-1} \text{ cm}^{-2} \text{ s}^{-1}$.

This paper has been typeset from a $\text{\TeX}/\text{\LaTeX}$ file prepared by the author.